

Large-Scale Fabrication of TiO<sub>2</sub> Hierarchical Hollow SpheresXiaoxu Li,<sup>†</sup> Yujie Xiong,<sup>‡</sup> Zhengquan Li,<sup>†</sup> and Yi Xie\*<sup>†</sup>

Nano-materials and Nano-chemistry, Hefei National Laboratory for Physical Sciences at Microscale, University of Science and Technology of China, Hefei, Anhui 230026, People's Republic of China, and Department of Chemistry, University of Washington, Seattle, Washington 98195-1700

Received February 14, 2006

In this Communication, we report the fabrication of well-crystallized rutile-phase TiO<sub>2</sub> hollow spheres using potassium titanium oxalate as the precursor. The spheres exhibited unique three-dimensional hierarchical architectures and demonstrated a significantly improved photocatalytic performance. The synthetic strategy used in this process represents a general approach and therefore may contribute to the formation mechanisms of hollow nanostructures.

In the past decade, the development of nanotechnology has made significant contributions to surface chemistry and catalysis.<sup>1</sup> To evaluate the dependence of the catalytic performance on their size, shape, composition, and crystallinity, various nanostructures have been synthesized. As photocatalysts that have been extensively investigated, TiO<sub>2</sub> nanoparticles are widely used in photovoltaic devices, gas sensors, and dye-sensitized solar cells because of their superior chemical properties.<sup>2</sup> To this end, a great deal of effort has been devoted to the synthesis of TiO<sub>2</sub> nanotubes, nanorods, nanowires, or shuttle-shape nanocrystals.<sup>3</sup> In comparison, the fabrication of well-crystallized TiO<sub>2</sub> hollow spheres remains a grand challenge.<sup>4</sup>

Recently, self-assembled hierarchical structures with hollow interiors have received much attention because of their

low density, high surface area, delivering ability, and surface permeability. For photocatalysts, the high-energy conversion efficiencies as well as large light-harvesting capacities can be achieved by constructing their complex architectures. Here we designed a bubble-template approach to generate well-crystallized self-assembled hierarchical structures of rutile-phase TiO<sub>2</sub> that are composed of small nanocrystals from a titanium oxo compound precursor. Thanks to their three-dimensional (3D) architecture, the photocatalytic performance of as-prepared hierarchical structures was significantly improved, compared with other shapes.

In a typical synthesis, 0.708 g (2 mmol) of potassium titanium oxalate (PTO) was dissolved in 15 mL of distilled water, followed by the addition of 15 mL of 30% H<sub>2</sub>O<sub>2</sub> and 1–2 mL of 37% HCl, which formed a characteristic dark-red solution. The solution was then transferred to a 50-mL Teflon-lined autoclave, which was filled with distilled water up to 90% of the total volume. The autoclave was sealed, heated at 150 °C for 8 h, and allowed to cool to room temperature naturally. The white precipitate was collected, washed with distilled water several times, and then dried in a vacuum at 60 °C for 6 h. The yield was around 94% (approximately 0.150 g).

The phase and purity of the product was determined by powder X-ray diffraction (XRD) analyses, which were carried out on a Rigaku D/max-γA X-ray diffractometer with Cu Kα radiation ( $\lambda = 1.54178 \text{ \AA}$ ). All of the observed peaks of the pattern in Figure 1 can be indexed to a pure tetragonal rutile phase (JCPDS card, 21-1276) with lattice constants  $a = 4.593 \text{ \AA}$  and  $c = 2.958 \text{ \AA}$ . No peak for other types was observed, showing the high purity and well crystallinity of the sample.

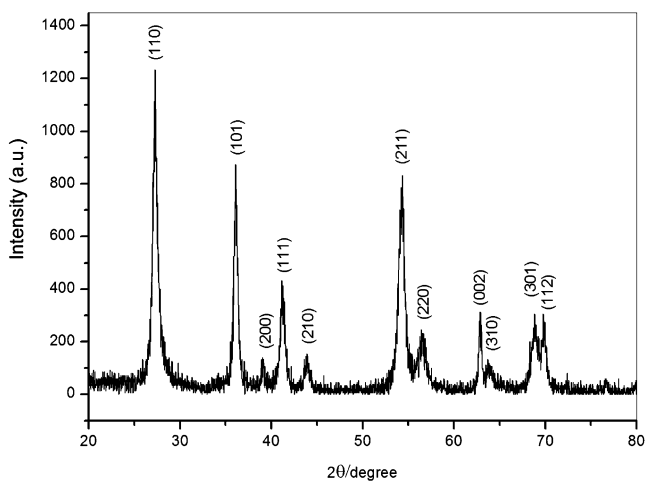
The morphology and structure of the product was then examined by a field emission scanning electron microscope (JEOL JSM-6700F SEM), a high-resolution transmission electron microscope (HRTEM, JEOL-2010), and selected-area electron diffraction (ED) at an acceleration voltage of 200 kV. Figure 2A shows a panoramic SEM image of the as-synthesized product. The sample mainly contains uniform hollow spheres with diameters of about 1 μm and a rough

\* To whom correspondence should be addressed. E-mail: yxie@ustc.edu.cn.

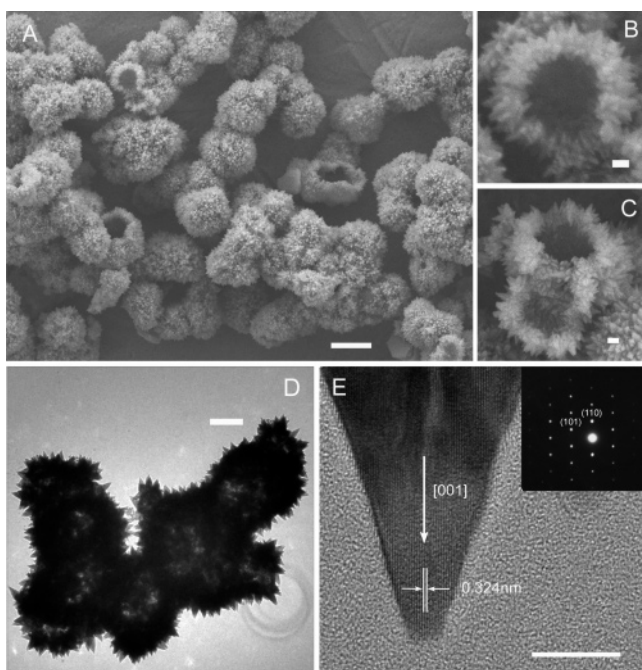
<sup>†</sup> University of Science and Technology of China.

<sup>‡</sup> University of Washington.

- (1) (a) Bell, A. T. *Science* **2003**, *299*, 1688. (b) Subramanian, V.; Wolf, E. E.; Kamat, P. V. *J. Am. Chem. Soc.* **2004**, *126*, 4943.
- (2) (a) Zhu, Y.; Shi, J.; Zhang, Z.; Zhang, C.; Zhang, X. *Anal. Chem.* **2000**, *35*, 3523. (b) O'Regan, B.; Gratzel, M. *Nature* **1991**, *353*, 737. (c) Nazerruddin, M. K.; Kay, A.; Rodicio, I.; Humphry-Baker, R.; Muller, E.; Liska, P.; Vlachopoulos, N.; Gratzel, M. *J. Am. Chem. Soc.* **1993**, *115*, 6382.
- (3) (a) Macak, J. M.; Tsuchiya, H.; Schmuki, P. *Angew. Chem., Int. Ed.* **2005**, *44*, 2100. (b) Jun, Y. W.; Casula, M. F.; Sim, J. H.; Kim, S. Y.; Cheon, J. W.; Alivisatos, A. P. *J. Am. Chem. Soc.* **2003**, *125*, 15981. (c) Kanie, K.; Sugimoto, T. *Chem. Commun.* **2004**, 1584.
- (4) (a) Yang, H. G.; Zeng, H. C. *J. Phys. Chem. B* **2004**, *108*, 3492. (b) Nakashima, T.; Kimizuka, N. *J. Am. Chem. Soc.* **2003**, *125*, 6386. (c) Collins, A. M.; Spickermann, C.; Mann, S. *J. Mater. Chem.* **2003**, *13*, 1112. (d) Zhong, Z. Y.; Yin, Y. D.; Gates, B.; Xia, Y. N. *Adv. Mater.* **2000**, *12*, 206.



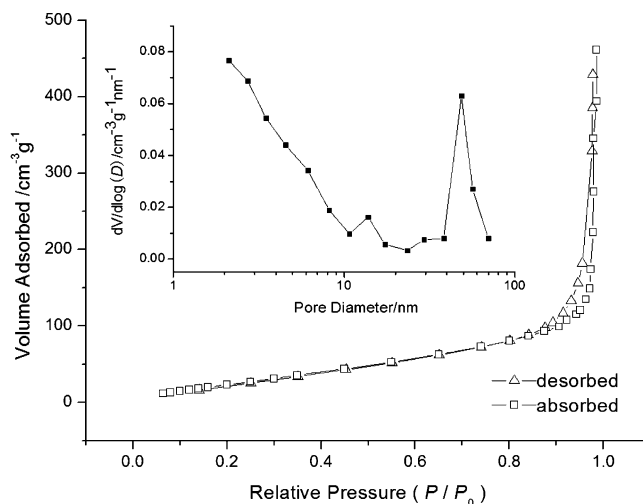
**Figure 1.** Powder XRD pattern of the as-synthesized hierarchical hollow spheres.



**Figure 2.** (A) Panoramic SEM images of the as-synthesized hierarchical hollow spheres after ultrasonic treatment for 15 min. (B) SEM image of a hollow sphere in part A with higher magnification. (C) SEM image of an unveiled sphere, which clearly indicates the hollow structure of the spheres. (D) TEM image of the as-synthesized hierarchical hollow spheres. (E) HRTEM image of the tip of a building unit. The inset shows its selected-area ED pattern. The scale bars of parts A–E are 1  $\mu\text{m}$ , 100 nm, 100 nm, 300 nm, and 10 nm, respectively.

surface. The SEM images with high magnification (Figure 2B,C) reveal that they are self-assembled hierarchical structures that are composed of rhombic building units. The details of their interior can be clearly observed by the image of a single broken sphere after being unveiled by ultrasonication (see Figure 2C). The hollow structure of the spheres can also be identified by a TEM image (Figure 2D). The HRTEM image and ED pattern (Figure 2E) reveal that the rhombic building units are single-crystal and grow along the [001] axis.

The hollow nature of the product was further confirmed by measurement of the pore-size distribution, which was obtained by the nitrogen adsorption–desorption isotherm and

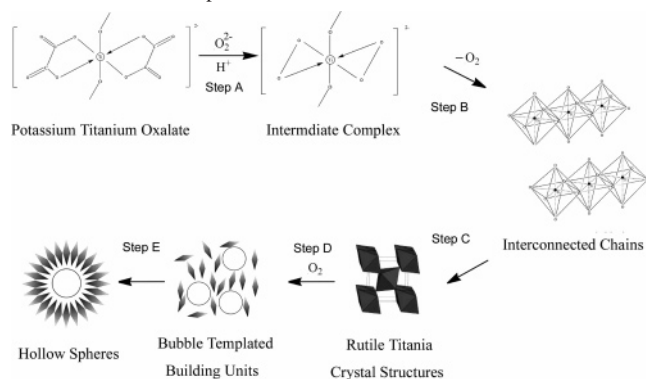


**Figure 3.** Nitrogen adsorption–desorption isotherm of  $\text{TiO}_2$  hierarchical hollow spheres. The inset is its BJH pore-size distribution curve.

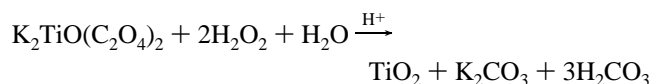
Barrett–Joyner–Halenda (BJH) methods on a Micromeritics ASAP 2000 accelerated surface area and porosimetry system. The isotherm can be categorized as type IV, with a distinct hysteresis loop observed in the range of 0.6–1.0  $P/P_0$  (Figure 3). The measurement shows that these spheres have pores with diameters of ca. 50 nm (Figure 3, inset) and that the Brunauer–Emmett–Teller (BET) surface area is 130.2  $\text{m}^2/\text{g}$ . The measured pore diameter is in good agreement with the value determined by SEM and TEM and shows that the building blocks are not tightly adhered to each other.

Traditionally, the synthesis of  $\text{TiO}_2$  involves hydrolyzation of titanium halides<sup>5</sup> or titanium alkoxides.<sup>6</sup> Because these precursors are small molecules, there is no motivation to construct well-organized 3D architectures while the titania form; as a result, the products are mainly random-arranged nanocrystals. In comparison, PTO represents a category of titanium oxo compounds.<sup>7</sup> As illustrated in Scheme 1, each Ti atom is coordinated by two  $[\text{C}_2\text{O}_4]^{2-}$  ions and bridged by two O atoms to form octahedral structures that are connected with each other. These characteristics enable us to build a complex architecture based on PTO molecules. In the synthesis presented here,  $[\text{C}_2\text{O}_4]^{2-}$  ions were attacked by exceeding  $\text{O}_2^{2-}$  ions under acidic hydrothermal conditions and subsequently replaced via a ligand-exchange reaction (step A). Formation of the intermediate complex was confirmed by the characteristic dark-red color. Then the complex decomposed and released  $\text{O}_2$  to form  $\text{TiO}_2$  octahedrons sharing edges (step B).<sup>8</sup> As a result, the rhombic crystals of rutile-phase  $\text{TiO}_2$  formed as a result of the oriented

- (5) (a) Niederberger, M.; Bartl, M. H.; Stucky, G. D. *Chem. Mater.* **2002**, *14*, 4364. (b) Cheng, H. M.; Ma, J. M.; Zhao, Z. G.; Qi, L. M. *Chem. Mater.* **1995**, *7*, 663. (c) Wang, W.; Gu, B. H.; Liang, L. Y.; Hamilton, W. A.; Wesolowski, D. J. *J. Phys. Chem. B* **2004**, *108*, 14789.
- (6) (a) Zhang, Z. H.; Zhong, X. H.; Liu, S. H.; Li, D. F.; Han, M. Y. *Angew. Chem., Int. Ed.* **2005**, *44*, 3466. (b) Cozzoli, P. D.; Kornowski, A.; Weller, H. *J. Am. Chem. Soc.* **2003**, *125*, 14539.
- (7) (a) Greenwood, N. N.; Earnshaw, A. *Chemistry of the Elements*; Butterworth-Heinemann Ltd.: Boston, MA, 1984. (b) Kolen'ko, Y. V.; Maximov, V. D.; Garshev, A. V.; Meskin, P. E.; Oleynikov, N. N.; Churagulov, B. R. *Chem. Phys. Lett.* **2004**, *388*, 411.
- (8) As is well-known, rutile-phase  $\text{TiO}_2$  is composed of edge-sharing octahedrons while anatase-phase  $\text{TiO}_2$  is composed of point-sharing ones. The model is well consistent with the XRD pattern.

**Scheme 1.** Schematic Illustration of the Formation Process of Hierarchical Hollow Spheres

growth along the [001] axis (step C). Because there are enough  $\text{O}_2$  bubbles decomposed from  $\text{H}_2\text{O}_2$  as soft templates, the self-assembly of rhombic crystallites driven by the interfacial energy minimization finally led to hierarchical hollow spheres (steps D and E). A similar gaseous bubble has also been used as a template for ZnO and ZnSe hollow nanostructures.<sup>9</sup> Note that in the reaction  $\text{H}_2\text{O}_2$  acted as both the coordination reagent and the bubble generator. Further experiments also lend support to this proposed mechanism. The present hierarchical structures could not be obtained using other nonvolatile oxidizers or coordination reagents. Moreover, the reaction temperatures as well as the amount of  $\text{H}_2\text{O}_2$ , which have significant effects on the pressure in the autoclave and affect the solubility of the gaseous bubbles, play important roles in determining the morphology of the spheres. We varied the temperature and ratio of  $\text{H}_2\text{O}_2/\text{H}_2\text{O}$  to reach a group of optimal conditions, as accounted in the Experimental Section. The overall reaction can be formulated as follows:



To evaluate the photocatalytic activity of our product, we compared it with other common samples. In a typical process, 10 mg of  $\text{TiO}_2$  hollow spheres was added to 100 mL of a  $1.0 \times 10^{-5}$  M Rhodamine B (RB) solution and then magnetically stirred in the dark for 15 min, which allowed it to reach adsorption equilibrium and uniform dispersity. The solution was then exposed to UV irradiation from a 250-W high-pressure Hg lamp at room temperature. The

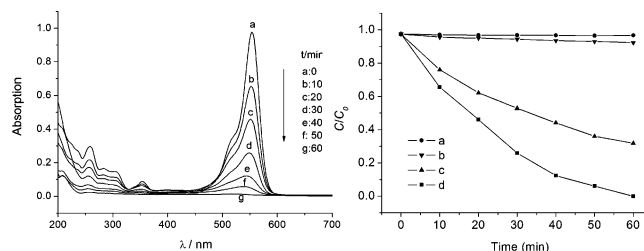


**Figure 4.** (A) Absorption spectra of a solution of RB ( $1.0 \times 10^{-5}$  M, 100 mL) in the presence of 10 mg of  $\text{TiO}_2$  hollow spheres under exposure to UV light. (B) Photocatalytic performances of various samples: (a) without UV irradiation; (b) without catalyst; (c) with rutile-phase  $\text{TiO}_2$  nanorods; (d) with rutile-phase  $\text{TiO}_2$  hollow spheres.

samples were collected by centrifugation every 10 min to measure the RB degradation by UV-vis spectra (Shimadzu UV2550). Figure 4A shows the evolution of RB absorption spectra in the presence of 10 mg of  $\text{TiO}_2$  hollow spheres, from which we can see that the concentration of RB decreased rapidly. We also used commercial Degussa P-25  $\text{TiO}_2$  and rutile-phase  $\text{TiO}_2$  nanorods (ca. 15 nm, BET 142.1  $\text{m}^2/\text{g}$ )<sup>10</sup> as references to evaluate the photocatalytic performance of our product. As illustrated in Figure 4B, we plotted the change in the concentration of RB under five different situations. Note that the concentration of RB was determined according to the characteristic peak at around 553 nm in the UV-vis spectra. It is obvious that our rutile-phase  $\text{TiO}_2$  hollow spheres exhibited superior photoactivities over rod-shaped nanocrystals, indicating that the generation of hierarchical hollow structures could improve their photocatalytic performance. Because of the drawback of its rutile phase on photocatalysis, the performance of our product is somewhat poorer than anatase-phase P-25, which is under expectation.

In summary, we have synthesized rutile-phase  $\text{TiO}_2$  hierarchical hollow spheres using PTO as the precursor. A bubble-template strategy is designed to construct the hollow nanostructure. The simple, general, clean, and convenient method presented here could generate desirable nanostructures with high purity and good crystallinity. Thanks to the 3D architecture of the product, the photocatalytic performance has been significantly improved. We believe that the present work will open up to systematically explore ways to fabricate hollow nanostructures and thus find use in a variety of applications.

**Acknowledgment.** This work was supported by the Chinese National Nature Science Foundation.

IC0602502

(9) (a) Zhang, J.; Sun, L. D.; Liao, C. S.; Yan, C. H. *Chem. Commun.* **2002**, 262. (b) Peng, Q.; Dong, Y. J.; Li, Y. D. *Angew. Chem., Int. Ed.* **2003**, 42, 3027.

(10) Huang, Q.; Gao, L. *Chem. Lett.* **2003**, 32, 638.